Satellites Spectral Information and Soil Organic Carbon

Subjects: Soil Science

Contributor: Emmanuelle Vaudour , Asa Gholizadeh , Fabio Castaldi , Mohammadmehdi Saberioon , Luboš Borůvka , Diego Urbina-Salazar , Youssef Fouad , Dominique Arrouays , Anne C. Richer-de-Forges , James Biney , Johanna Wetterlind , Bas Van Wesemael

There is a need to update soil maps and monitor soil organic carbon (SOC) in the upper horizons or plough layer for enabling decision support and land management, while complying with several policies, especially those favoring soil carbon storage. A number of satellite-based spectral approaches for SOC assessment have been achieved from several satellite sensors, study scales and geographical contexts in the past decade.

soil organic carbon spectral models satellite imagery

1. Satellites Spectral Information

Since 1972, i.e., the very beginning of the civilian satellite remote sensing, until the mid-2010s, satellite data available in the optical domain were mostly acquired from multispectral sensors, i.e., sensors with a discrete number of spectral bands. Most historical data were obtained over wide swaths by the Landsat satellites equipped with Thematic Mapper (TM), Enhanced Thematic Mapper (ETM+), and, more recently, Landsat 8 Operational Land Imager (OLI) sensors with 30 m resolution. Additionally, data from the *Satellite Pour l'Observation de la Terre* (SPOT) equipped with the sensor *Haute Résolution Visible* (HRV) with 20 m resolution were found dating back to 1986. Some pioneering studies about topsoil SOC content detection from satellite data have been carried out, for instance, considering SPOT HRV bands [1][2][3] or Landsat bands [4][5][6].

Since 2000, hyperspectral satellite images have been made available from the Hyperion sensor with 30 m resolution onboard the satellite Earth Observing 1 (2000–2017), and from the Compact High-Resolution Imaging Spectrometer (CHRIS) with 17 m resolution onboard the Project for On-Board Autonomy (PROBA-1) micro-satellite (2001–ongoing). Since 2019, the *PRecursore IperSpettrale della Missione Applicativa* (PRISMA) with 239 spectral bands between 400 and 2505 nm has delivered images with 30 m resolution [7]. Approaches of satellite-based SOC modeling have been carried out from Hyperion [8][9][10], CHRIS-PROBA [11], simulated PRISMA [12] and PRISMA [13]. As the Environmental Mapping and Analysis Program (EnMAP) [14] was just launched on 1 April 2022 and is currently in the commissioning phase, some studies have considered simulated EnMAP for the assessment of SOC content [15][16] till actual EnMAP data becomes available. To our knowledge, no reference was found about simulated spectra for other forthcoming hyperspectral satellites such as CHIME, SHALOM or HypXim. Some recent Chinese studies used the hyperspectral data of the Gaofen-5 satellite with a 30 m resolution and bandwidth of 60 km [17][18][19]. In parallel, with the emerging of precision agriculture, field-scale approaches to SOC modeling have also been developed from satellite sensors with higher spatial resolution: IKONOS with 4 m resolution [20], PlanetScope with 3 m resolution [21] and Worldview 2 with 2.5 m resolution [22][23].

Since 2015 and then 2017, when Sentinel-2A, followed by Sentinel-2B were launched, the Sentinel-2 (S2) time-series equipped with the MultiSpectral Instrument (MSI, 13 spectral bands) provided not only wide spatial coverage over swaths of 290 km, but also 10 to 20 m resolution (10 spectral bands) and a 5-day revisit. The advent of such time-series favored the renewal of the satellite-derived spectral models and particularly for SOC, using either single date acquisitions [21][24][25][26][27][28][29][30][31][32] or multi-date approaches [13][33][34][35][36]. In addition, some authors used Sentinel-1 synthetic aperture radar (SAR) images in their approach, either separately [27][32][35] or directly as covariates within their modeling [32][37]. Over very large areas or at national scales, other authors used coarse resolution satellite series, being either MODIS with 250 or 500 m resolution [38][39] or Sentinel-3 equipped with the Ocean and Land Colour Instrument (OLCI) with 300 m resolution [40].

2. Overall Characteristics of Soil Data

2.1. Soil Types and Agroecosystems under Study

Most approaches relying on pure spectral models have been carried out since 2019 and have dealt with temperate croplands in Europe, China and North America, with few in Mediterranean [11][12][26][41] and arid environments [6][42][43] and even fewer in tropical ecosystems [4][36][44][45] (**Figure 1**).

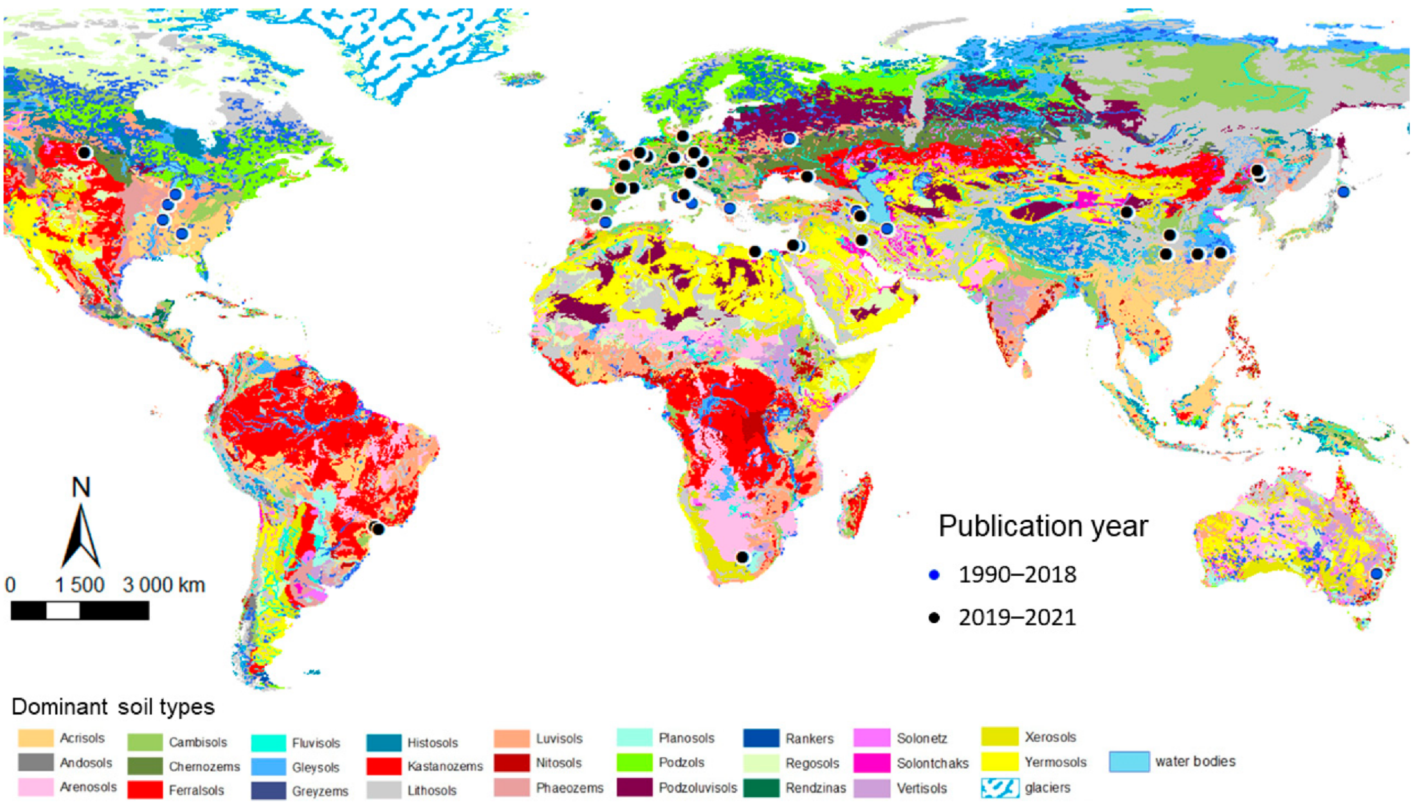

Figure 2. World map of satellite-derived SOC studies and the dominant soil types of the FAO-UNESCO Digital Soil Map of the World at 1:5.000.000 scale [46]. Time spans are split according to the first year of Sentinel-2 based SOC studies, i.e., 2018.

Most studies were in rainfed annual cropping systems with very few studies in vineyards and even fewer in orchards. It should be noted that information on management practices or soil surface conditions was scarce.

Soil types refer to the World Reference Base (WRB) [47] in most cases, although the US Soil Taxonomy [48] was also used. The soils are typically cambisols and luvisols and, to a lesser extent, regosols, leptosols, stagnosols, chernozems and the so-called “inceptisols” of the US Soil Taxonomy (mostly equivalent to cambisols) (**Figure 2**). The most frequent qualifier is “haplic”. The “calcaric” qualifier is not dominant, and therefore calcium carbonate contents can be assumed to be low.

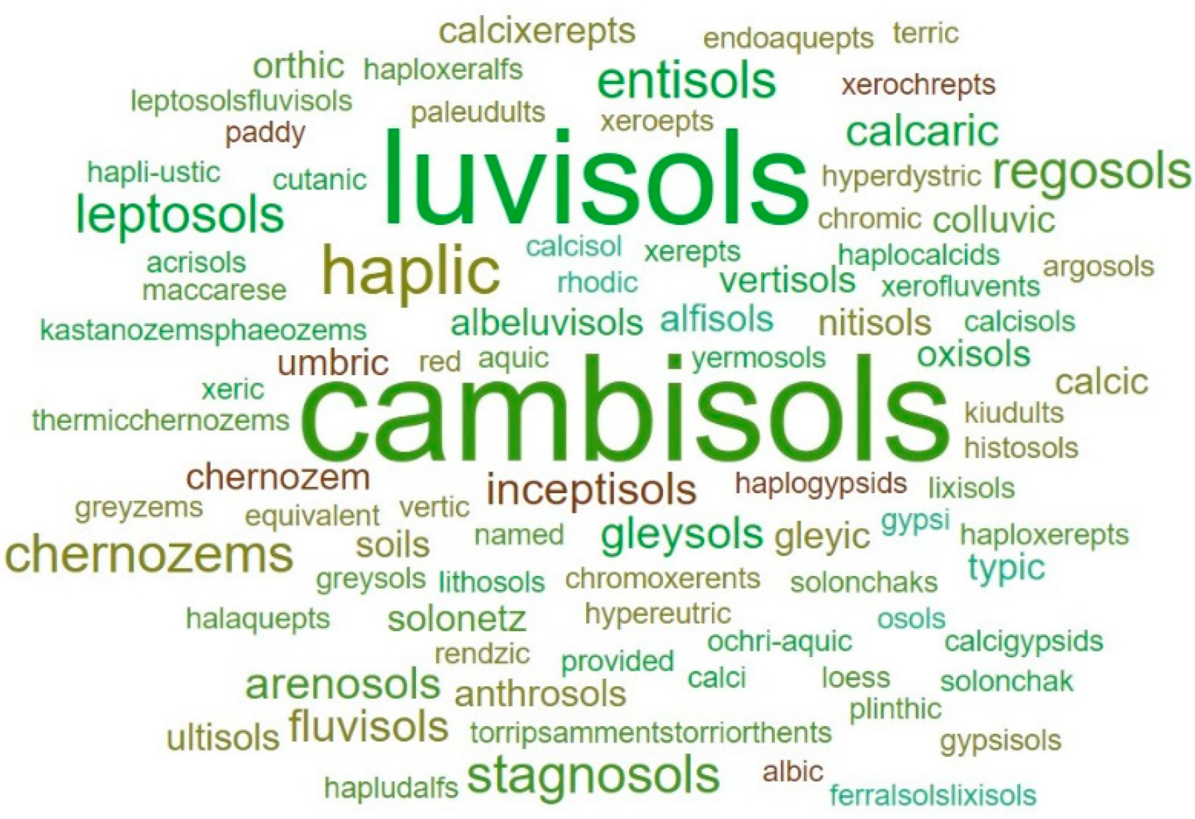

Figure 2. Word cloud of soil types considered in satellite-derived SOC published studies (word size varies with frequency).

2.2. Spatial Scales, Sample Size and Density

Most studies were carried out at the scale of small regions, of some hundreds of km^2: study areas covered a median of 118 km^2 (**Figure 3**). The sample density for small regions ranged between 0.1 and 16.1 samples per km^2, with a mean value of 2.7 samples per km^2. For large regions (up to 10,000 km^2) and very large regions (>10,000 km^2 and up to 150,000 km^2), the mean sample density was lower than or equal to 0.1 samples per km^2, while it was higher than or equal to 201 for farm- or field-scale studies. The total sample size ranged from 32 to 1753 topsoil samples, most of them being collected from the 0–10 cm or 0–20 cm topsoil. The median sample size varies from 85 for field and farm, to 100 for small regions, 264 for large regions and reaches 625 samples for very large regions.

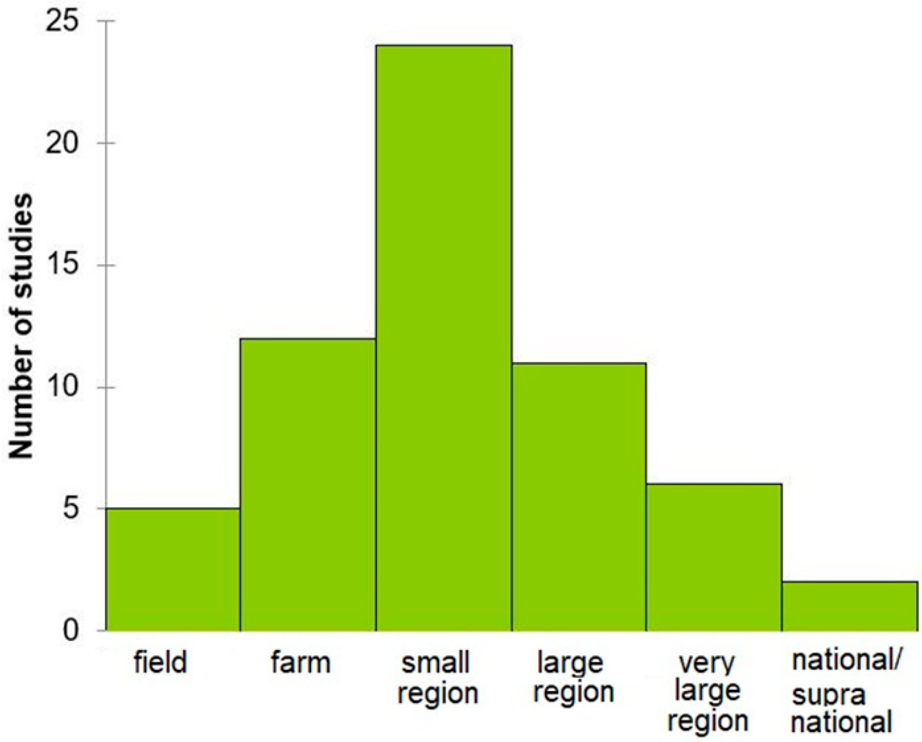

Figure 3. Histogram of study scales considered in satellite-derived SOC studies.

2.3. Ranges of SOC Considered and the Issue of Standard Lab Determinations

Table 1 sheds light on the basic statistics of topsoil SOC considered in the selected studies. The datasets of measured topsoil SOC contents refer to mineral soils with annual crop systems with an average value of ~15 g·kg^{-1} and a range of 30 g·kg^{-1} in median.

Table 1. Basics stats of topsoil SOC content values (top SOC, g·kg^{-1}) across 46 study areas with full description of measured sampled sets [3][8][11][12][13][18][21][24][25][26][27][29][31][32][34][35][38][41][44][49][50][51][52][53][54][55][56][57][58][59][60], q1, first quartile; μ, mean; q3; third quartile; σ, standard deviation.

Statistic	Min	q1	μ	q3	Max	σ	Median
Minimum top SOC	0.0	2.7	5.8	6.9	26.1	4.7	6.0
Maximum top SOC	10.0	21.8	82.7	115.8	439.0	102.0	37.3
Top SOC range	4.6	17.8	76.9	110.7	438.4	103.0	30.0
Average top SOC	1.7	12.6	17.4	19.6	50.0	9.5	15.1

Mineral and organic soils are usually processed separately, but the threshold between these categories is not uniform: at the scale of the USA, Wang et al. [61] chose to discriminate between mineral and organic soils using the threshold of 120 g·kg^{-1}.

As the analytical methods used for SOC measurements are far from being homogeneous among laboratories and countries, and specifically in the context of the satellite-derived SOC studies, the basic stats displayed in **Table 1** should be considered with caution. Dry combustion was used for 50% of the studies and wet oxidation for 30%, while analytical methods were simply not specified for the remaining studies. Historically, one of the most-used methods has been the Walkley–Black method [62] using wet oxidation. This method is still being used in numerous countries, and several modified methods based on the same principles have also been proposed, e.g., [63][64][65][66]. The underestimation of the total SOC content caused by a reduced wet oxidation of the more stable or "recalcitrant" fractions of SOC is the major limitation of this method.

The modern standard method, supposed to be the reference, is dry combustion coupled with an automated CHN analyzer. Automated dry combustion (ADC) involves measurements of SOC based on CO_2 released from thermally oxidized soil [67]. Therefore, a recovery factor must be used to convert the results from the wet oxidation to the dry combustion method. The most frequently used correction factor is 1.33 [68]. However, a careful look at the literature [68][69][70][71][72] shows that the recovery factors cover a wide range (1 to 1.8) depending on climate, soil types, depth, texture, and the relative proportion of various SOC constituents. Moreover, CN analyzers determine total carbon, i.e., SOC and carbonates. Thus, the SOC content of calcareous samples is determined by subtracting carbon content from carbonates to total carbon content, e.g., [73].

Other standard methods that were not found among the satellite-derived SOC studies include various adaptations of the Mehlich method [74] that aim at extracting humic substances, or loss-on-ignition [67][75], the latter being mainly used for the organic horizons.

All methods have some drawbacks, and the less biased one is ADC, with some exceptions for very organic soils. One consequence is that when using SOC data, and especially when compiling legacy SOC data, metadata should include the laboratory method. Another consequence is that there is no universal factor to convert the results from one method to another, and that such a conversion needs to be locally adapted. Finally, any change of method between two dates may lead to false conclusions about SOC changes.

Moreover, over the past decade, laboratory spectroscopic measurements have been successfully tested to predict SOC contents over the visible near-infrared and shortwave infrared ranges [76][77][78][79], in combination with UV-visible fluorescence measurements [80] or restricted to the visible range only [81], or over the mid-infrared only (4000–400 cm^{-1}) [82]. An emergent technology is also laser-induced breakdown spectroscopy, e.g., [83]. These low-cost technologies are good candidates to provide numerous training information for digital soil mapping (DSM). However, the uncertainty of these measurements often remains a limitation, if the aim is to detect small changes in SOC with time. One emerging promising method is analyzing SOC with Rock-Eval analyses [84], which would pave the way to both estimating total SOC and indicators of its sensibility to mineralization and its potential for long-term sequestration in soils.

References

1. Agbu, P.A.; Fehrenbacher, D.J.; Jansen, I.J. Soil Property Relationships with SPOT Satellite Digital Data in East Central Illinois. Soil Sci. Soc. Am. J. 1990, 54, 807–812.
2. Berthier, L.; Pitres, J.C.; Vaudour, E. Prédiction spatiale des teneurs en carbone organique des sols par spectroscopie visible-proche infrarouge et télédétection satellitale SPOT. Exemple au niveau d’un périmètre d’alimentation en eau potable en Beauce. Etude Gest. Sols 2008, 15, 161–172.
3. Vaudour, E.; Bel, L.; Gilliot, J.M.; Coquet, Y.; Hadjar, D.; Cambier, P.; Michelin, J.; Houot, S. Potential of SPOT Multispectral Satellite Images for Mapping Topsoil Organic Carbon Content over Peri-Urban Croplands. Soil Sci. Soc. Am. J. 2013, 77, 2122.
4. Nanni, M.R.; Demattê, J.A.M. Spectral Reflectance Methodology in Comparison to Traditional Soil Analysis. Soil Sci. Soc. Am. J. 2006, 70, 393–407.
5. Huang, X.; Senthilkumar, S.; Kravchenko, A.; Thelen, K.; Qi, J. Total carbon mapping in glacial till soils using near-infrared spectroscopy, Landsat imagery and topographical information. Geoderma 2007, 141, 34–42.
6. Jarmer, T.; Hill, J.; Lavée, H.; Sarah, P. Mapping Topsoil Organic Carbon in Non-agricultural Semi-arid and Arid Ecosystems of Israel. Photogramm. Eng. Remote Sens. 2010, 76, 85–94.
7. Loizzo, R.; Guarini, R.; Longo, F.; Scopa, T.; Formaro, R.; Facchinetti, C.; Varacalli, G. Prisma: The Italian hyperspectral mission. In Proceedings of the IGARSS 2018—2018 IEEE International Geoscience and Remote Sensing Symposium, Valencia, Spain, 22–27 July 2018; pp. 175–178.
8. Gomez, C.; Viscarra Rossel, R.A.; McBratney, A.B. Soil Organic Carbon Prediction by Hyperspectral Remote Sensing and Field Vis-NIR Spectroscopy: An Australian Case Study. Geoderma 2008, 146, 403–411.
9. Jaber, S.M.; Lant, C.L.; Al-Qinna, M.I. Estimating spatial variations in soil organic carbon using satellite hyperspectral data and map algebra. Int. J. Remote Sens. 2011, 32, 5077–5103.
10. Nowkandeh, S.M.; Homaee, M.; Noroozi, A.A. Mapping Soil Organic Matter Using Hyperion Images. Int. J. Agron. Plant Prod. 2013, 4, 1753–1759.
11. Casa, R.; Castaldi, F.; Pascucci, S.; Basso, B.; Pignatti, S. Geophysical and Hyperspectral Data Fusion Techniques for In-Field Estimation of Soil Properties. Vadose Zone J. 2013, 12, 1–10.

12. Castaldi, F.; Palombo, A.; Santini, F.; Pascucci, S.; Pignatti, S.; Casa, R. Evaluation of the potential of the current and forthcoming multispectral and hyperspectral imagers to estimate soil texture and organic carbon. Remote Sens. Environ. 2016, 179, 54–65.
13. Mzid, N.; Castaldi, F.; Tolomio, M.; Pascucci, S.; Casa, R.; Pignatti, S. Evaluation of Agricultural Bare Soil Properties Retrieval from Landsat 8, Sentinel-2 and PRISMA Satellite Data. Remote Sens. 2022, 14, 714.
14. Guanter, L.; Kaufmann, H.; Segl, K.; Foerster, S.; Rogass, C.; Chabrillat, S.; Kuester, T.; Hollstein, A.; Rossner, G.; Chlebek, C.; et al. The EnMAP Spaceborne Imaging Spectroscopy Mission for Earth Observation. Remote Sens. 2015, 7, 8830–8857.
15. Steinberg, A.; Chabrillat, S.; Stevens, A.; Segl, K.; Foerster, S. Prediction of Common Surface Soil Properties Based on Vis-NIR Airborne and Simulated EnMAP Imaging Spectroscopy Data: Prediction Accuracy and Influence of Spatial Resolution. Remote Sens. 2016, 8, 613.
16. Ward, K.J.; Chabrillat, S.; Brell, M.; Castaldi, F.; Spengler, D.; Foerster, S. Mapping Soil Organic Carbon for Airborne and Simulated EnMAP Imagery Using the LUCAS Soil Database and a Local PLSR. Remote Sens. 2020, 12, 3451.
17. Meng, X.; Bao, Y.; Liu, J.; Liu, H.; Zhang, X.; Zhang, Y.; Wang, P.; Tang, H.; Kong, F. Regional soil organic carbon prediction model based on a discrete wavelet analysis of hyperspectral satellite data. Int. J. Appl. Earth Obs. Geoinf. 2020, 89, 102111.
18. Meng, X.; Bao, Y.; Ye, Q.; Liu, H.; Zhang, X.; Tang, H.; Zhang, X. Soil Organic Matter Prediction Model with Satellite Hyperspectral Image Based on Optimized Denoising Method. Remote Sens. 2021, 13, 2273.
19. Bao, Y.; Ustin, S.; Meng, X.; Zhang, X.; Guan, H.; Qi, B.; Liu, H. A Regional-Scale Hyperspectral Prediction Model of Soil Organic Carbon Considering Geomorphic Features. Geoderma 2021, 403, 115263.
20. Sullivan, D.G.; Shaw, J.N.; Rickman, D. IKONOS Imagery to Estimate Surface Soil Property Variability in Two Alabama Physiographies. Soil Sci. Soc. Am. J. 2005, 69, 1789–1798.
21. Žížala, D.; Minařík, R.; Zádorová, T. Soil Organic Carbon Mapping Using Multispectral Remote Sensing Data: Prediction Ability of Data with Different Spatial and Spectral Resolutions. Remote Sens. 2019, 11, 2947.
22. Stamatiadis, S.; Evangelou, L.; Blanta, A.; Tsadilas, C.; Tsitouras, A.; Chroni, C.; Christophides, C.; Tsantila, E.; Samaras, V.; Dalezios, N.; et al. Satellite Visible–Near Infrared Reflectance Correlates to Soil Nitrogen and Carbon Content in Three Fields of the Thessaly Plain (Greece). Commun. Soil Sci. Plant Anal. 2013, 44, 28–37.
23. Samsonova, V.P.; Meshalkina, J.L.; Blagoveschensky, Y.N.; Yaroslavtsev, A.M.; Stoorvogel, J.J. The Role of Positional Errors While Interpolating Soil Organic Carbon Contents Using Satellite

Imagery. Precis. Agric. 2018, 19, 1085–1099.

24. Gholizadeh, A.; Žižala, D.; Saberioon, M.; Borůvka, L. Soil organic carbon and texture retrieving and mapping using proximal, airborne and Sentinel-2 spectral imaging. Remote Sens. Environ. 2018, 218, 89–103.
25. Castaldi, F.; Hueni, A.; Chabrillat, S.; Ward, K.; Buttafuoco, G.; Bomans, B.; Vreys, K.; Brell, M.; van Wesemael, B. Evaluating the capability of the Sentinel 2 data for soil organic carbon prediction in croplands. ISPRS J. Photogramm. Remote Sens. 2019, 147, 267–282.
26. Vaudour, E.; Gomez, C.; Fouad, Y.; Lagacherie, P. Sentinel-2 image capacities to predict common topsoil properties of temperate and Mediterranean agroecosystems. Remote Sens. Environ. 2019, 223, 21–33.
27. Vaudour, E.; Gomez, C.; Loiseau, T.; Baghdadi, N.; Loubet, B.; Arrouays, D.; Ali, L.; Lagacherie, P. The Impact of Acquisition Date on the Prediction Performance of Topsoil Organic Carbon from Sentinel-2 for Croplands. Remote Sens. 2019, 11, 2143.
28. Dvorakova, K.; Shi, P.; Limbourg, Q.; van Wesemael, B. Soil Organic Carbon Mapping from Remote Sensing: The Effect of Crop Residues. Remote Sens. 2020, 12, 1913.
29. Zhou, T.; Geng, Y.; Chen, J.; Liu, M.; Haase, D.; Lausch, A. Mapping soil organic carbon content using multi-source remote sensing variables in the Heihe River Basin in China. Ecol. Indic. 2020, 114, 106288.
30. Biney, J.K.M.; Saberioon, M.; Borůvka, L.; Houška, J.; Vašát, R.; Chapman Agyeman, P.; Coblinski, J.A.; Klement, A. Exploring the Suitability of UAS-Based Multispectral Images for Estimating Soil Organic Carbon: Comparison with Proximal Soil Sensing and Spaceborne Imagery. Remote Sens. 2021, 13, 308.
31. Wang, K.; Qi, Y.; Guo, W.; Zhang, J.; Chang, Q. Retrieval and Mapping of Soil Organic Carbon Using Sentinel-2A Spectral Images from Bare Cropland in Autumn. Remote Sens. 2021, 13, 1072.
32. Urbina-Salazar, D.; Vaudour, E.; Baghdadi, N.; Ceschia, E.; Richer-de-Forges, A.C.; Lehmann, S.; Arrouays, D. Using Sentinel-2 Images for Soil Organic Carbon Content Mapping in Croplands of Southwestern France. The Usefulness of Sentinel-1/2 Derived Moisture Maps and Mismatches between Sentinel Images and Sampling Dates. Remote Sens. 2021, 13, 5115.
33. Dvorakova, K.; Heiden, U.; van Wesemael, B. Sentinel-2 Exposed Soil Composite for Soil Organic Carbon Prediction. Remote Sens. 2021, 13, 1791.
34. Castaldi, F. Sentinel-2 and Landsat-8 Multi-Temporal Series to Estimate Topsoil Properties on Croplands. Remote Sens. 2021, 13, 3345.
35. Vaudour, E.; Gomez, C.; Lagacherie, P.; Loiseau, T.; Baghdadi, N.; Urbina-Salazar, D.; Loubet, B.; Arrouays, D. Temporal mosaicking approaches of Sentinel-2 images for extending topsoil organic

carbon content mapping in croplands. Int. J. Appl. Earth Obs. Geoinf. 2021, 96, 102277.

36. Silvero, N.E.Q.; Demattê, J.A.M.; Amorim, M.T.A.; dos Santos, N.V.; Rizzo, R.; Safanelli, J.L.; Poppiel, R.R.; de Sousa Mendes, W.; Bonfatti, B.R. Soil Variability and Quantification Based on Sentinel-2 and Landsat-8 Bare Soil Images: A Comparison. Remote Sens. Environ. 2021, 252, 112117.
37. Wang, H.; Zhang, X.; Wu, W.; Liu, H. Prediction of Soil Organic Carbon under Different Land Use Types Using Sentinel-1/-2 Data in a Small Watershed. Remote Sens. 2021, 13, 1229.
38. Dou, X.; Wang, X.; Liu, H.; Zhang, X.; Meng, L.; Pan, Y.; Yu, Z.; Cui, Y. Prediction of soil organic matter using multi-temporal satellite images in the Songnen Plain, China. Geoderma 2019, 356, 113896.
39. Sothe, C.; Gonsamo, A.; Arabian, J.; Snider, J. Large Scale Mapping of Soil Organic Carbon Concentration with 3D Machine Learning and Satellite Observations. Geoderma 2022, 405, 115402.
40. Odebiri, O.; Mutanga, O.; Odindi, J. Deep Learning-Based National Scale Soil Organic Carbon Mapping with Sentinel-3 Data. Geoderma 2022, 411, 115695.
41. Tziolas, N.; Tsakiridis, N.; Ogen, Y.; Kalopesa, E.; Ben-Dor, E.; Theocharis, J.; Zalidis, G. An integrated methodology using open soil spectral libraries and Earth Observation data for soil organic carbon estimations in support of soil-related SDGs. Remote Sens. Environ. 2020, 244, 111793.
42. Jaber, S.M.; Al-Qinna, M.I. Global and local modeling of soil organic carbon using Thematic Mapper data in a semi-arid environment. Arab. J. Geosci. 2015, 8, 3159–3169.
43. Mohamed, E.S.; Baroudy, A.A.E.; El-Beshbeshy, T.; Emam, M.; Belal, A.A.; Elfadaly, A.; Aldosari, A.A.; Ali, A.M.; Lasaponara, R. Vis-NIR Spectroscopy and Satellite Landsat-8 OLI Data to Map Soil Nutrients in Arid Conditions: A Case Study of the Northwest Coast of Egypt. Remote Sens. 2020, 12, 3716.
44. Urbina-Salazar, D.F.; Demattê, J.A.M.; Vicente, L.E.; Guimarães, C.C.B.; Sayão, V.M.; Cerri, C.E.P.; Padilha, M.C.d.C.; Mendes, W.D.S. Emissivity of agricultural soil attributes in southeastern Brazil via terrestrial and satellite sensors. Geoderma 2020, 361, 114038.
45. Silvero, N.E.Q.; Demattê, J.A.M.; de Souza Vieira, J.; de Oliveira Mello, F.A.; Amorim, M.T.A.; Poppiel, R.R.; de Sousa Mendes, W.; Bonfatti, B.R. Soil Property Maps with Satellite Images at Multiple Scales and Its Impact on Management and Classification. Geoderma 2021, 397, 115089.
46. UNESCO. Digital Soil Map of the World; Legend: ; UNESCO: Paris, France, 1974; ISBN 978-92-3-101125-2. Available online: https://storage.googleapis.com/fao-maps-catalog-data/uuid/446ed430-8383-11db-b9b2-000d939bc5d8/resources/DSMW.zip (accessed on 13 May 2022).

47. Food and Agriculture Organization of the United Nations. World Reference Base for Soil Resources 2014: International Soil Classification System for Naming Soils and Creating Legends for Soil Maps; FAO: Rome, Italy, 2014; ISBN 978-92-5-108370-3.
48. Soil Survey Staff. Soil Taxonomy: A Basic System of Soil Classification for Making and Interpreting Soil Surveys, 2nd ed.; Natural Resources Conservation Service, U.S. Department of Agriculture Handbook; USDA: Washington, DC, USA, 1999; 436p. Available online: https://www.nrcs.usda.gov/wps/portal/nrcs/main/soils/survey/class/taxonomy/ (accessed on 13 May 2022).
49. Girard, M.-C. Emploi de la télédétection pour l'étude de l'humidité des sols. Houille Blanche 1978, 64, 533–539.
50. Liu, T.; Zhang, H.; Shi, T. Modeling and Predictive Mapping of Soil Organic Carbon Density in a Small-Scale Area Using Geographically Weighted Regression Kriging Approach. Sustainability 2020, 12, 9330.
51. Matinfar, H.R.; Maghsodi, Z.; Mousavi, S.R.; Rahmani, A. Evaluation and Prediction of Topsoil organic carbon using Machine learning and hybrid models at a Field-scale. CATENA 2021, 202, 105258.
52. Zepp, S.; Heiden, U.; Bachmann, M.; Wiesmeier, M.; Steininger, M.; van Wesemael, B. Estimation of Soil Organic Carbon Contents in Croplands of Bavaria from SCMaP Soil Reflectance Composites. Remote Sens. 2021, 13, 3141.
53. Wang, X.; Zhang, Y.; Atkinson, P.M.; Yao, H. Predicting soil organic carbon content in Spain by combining Landsat TM and ALOS PALSAR images. Int. J. Appl. Earth Obs. Geoinf. 2020, 92, 102182.
54. Safanelli, J.L.; Chabrillat, S.; Ben-Dor, E.; Demattê, J.A.M. Multispectral Models from Bare Soil Composites for Mapping Topsoil Properties over Europe. Remote Sens. 2020, 12, 1369.
55. Castaldi, F.; Chabrillat, S.; Don, A.; van Wesemael, B. Soil Organic Carbon Mapping Using LUCAS Topsoil Database and Sentinel-2 Data: An Approach to Reduce Soil Moisture and Crop Residue Effects. Remote Sens. 2019, 11, 2121.
56. Sorenson, P.T.; Shirtliffe, S.J.; Bedard-Haughn, A.K. Predictive soil mapping using historic bare soil composite imagery and legacy soil survey data. Geoderma 2021, 401, 115316.
57. Zhou, T.; Geng, Y.; Chen, J.; Pan, J.; Haase, D.; Lausch, A. High-resolution digital mapping of soil organic carbon and soil total nitrogen using DEM derivatives, Sentinel-1 and Sentinel-2 data based on machine learning algorithms. Sci. Total Environ. 2020, 729, 138244.
58. He, X.; Yang, L.; Li, A.; Zhang, L.; Shen, F.; Cai, Y.; Zhou, C. Soil organic carbon prediction using phenological parameters and remote sensing variables generated from Sentinel-2 images. CATENA 2021, 205, 105442.

59. Fathololoumi, S.; Vaezi, A.R.; Alavipanah, S.K.; Ghorbani, A.; Saurette, D.; Biswas, A. Improved digital soil mapping with multitemporal remotely sensed satellite data fusion: A case study in Iran. Sci. Total Environ. 2020, 721, 137703.

60. Mirzaee, S.; Ghorbani-Dashtaki, S.; Mohammadi, J.; Asadi, H.; Asadzadeh, F. Spatial variability of soil organic matter using remote sensing data. CATENA 2016, 145, 118–127.

61. Wang, S.; Guan, K.; Zhang, C.; Lee, D.; Margenot, A.J.; Ge, Y.; Peng, J.; Zhou, W.; Zhou, Q.; Huang, Y. Using Soil Library Hyperspectral Reflectance and Machine Learning to Predict Soil Organic Carbon: Assessing Potential of Airborne and Spaceborne Optical Soil Sensing. Remote Sens. Environ. 2022, 271, 112914.

62. Walkley, A.; Black, I.A. An Examination of the Degtjareff Method for Determining Soil Organic Matter, and a Proposed Modification of the Chromic Acid Titration Method. Soil Sci. 1934, 37, 29–38.

63. Anne, P. Sur le dosage du carbone organique du sol. Ann. Agron. 1945, 15, 161–172.

64. Walkley, A. A Critical Examination of a Rapid Method for Determining Organic Carbon in Soils—Effect of Variations in Digestion Conditions and of Inorganic Soil Constituents. Soil Sci. 1947, 63, 251–264.

65. Nelson, D.W.; Sommers, L.E. Total Carbon, Organic Carbon, and Organic Matter. In Methods of Soil Analysis Part 3—Chemical Methods; Sparks, D.L., Page, A.L., Helmke, P.A., Loeppert, R.H., Soltanpour, P.N., Tabatabai, M.A., Johnston, C.T., Summer, M.E., Eds.; Soil Science Society of America: Madison, WI, USA; American Society of Agronomy: Madison, WI, USA, 1996; pp. 961–1010.

66. Schumacher, B.A. Methods for the Determination of Total Organic Carbon (TOC) in Soils and Sediments; Ecological Risk Assessment Support Center, U.S. Environmental Protection Agency: Washington, DC, USA, 2002; 23p.

67. Abella, S.R.; Zimmer, B.W. Estimating Organic Carbon from Loss-On-Ignition in Northern Arizona Forest Soils. Soil Sci. Soc. Am. J. 2007, 71, 545–550.

68. Meersmans, J.; Van Wesemael, B.; Van Molle, M. Determining Soil Organic Carbon for Agricultural Soils: A Comparison between the Walkley & Black and the Dry Combustion Methods (North Belgium). Soil Use Manag. 2009, 25, 346–353.

69. Jolivet, C.; Arrouays, D.; Bernoux, M. Comparison between Analytical Methods for Organic Carbon and Organic Matter Determination in Sandy Spodosols of France. Commun. Soil Sci. Plant Anal. 1998, 29, 2227–2233.

70. De Vos, B.; Lettens, S.; Muys, B.; Deckers, J.A. Walkley-Black Analysis of Forest Soil Organic Carbon: Recovery, Limitations and Uncertainty. Soil Use Manag. 2007, 23, 221–229.

71. Chatterjee, A.; Lal, R.; Wielopolski, L.; Martin, M.Z.; Ebinger, M.H. Evaluation of Different Soil Carbon Determination Methods. Crit. Rev. Plant Sci. 2009, 28, 164–178.

72. Roper, W.R.; Robarge, W.P.; Osmond, D.L.; Heitman, J.L. Comparing Four Methods of Measuring Soil Organic Matter in North Carolina Soils. Soil Sci. Soc. Am. J. 2019, 83, 466–474.

73. AFNOR. Qualité des Sols; AFNOR: Paris, France; Eyrolles: Paris, France, 1999; Volume 1, 565p.

74. Mehlich, A. Photometric Determination of Humic Matter in Soils, a Proposed Method. Commun. Soil Sci. Plant Anal. 1984, 15, 1417–1422.

75. Ball, D.F. Loss-on-Ignition as an Estimate of Organic Matter and Organic Carbon in Non-Calcareous Soils. J. Soil Sci. 1964, 15, 84–92.

76. Wetterlind, J.; Stenberg, B. Near-Infrared Spectroscopy for within-Field Soil Characterization: Small Local Calibrations Compared with National Libraries Spiked with Local Samples. Eur. J. Soil Sci. 2010, 61, 823–843.

77. Grinand, C.; Barthès, B.G.; Brunet, D.; Kouakoua, E.; Arrouays, D.; Jolivet, C.; Caria, G.; Bernoux, M. Prediction of Soil Organic and Inorganic Carbon Contents at a National Scale (France) Using Mid-Infrared Reflectance Spectroscopy (MIRS). Eur. J. Soil Sci. 2012, 63, 141–151.

78. Gomez, C.; Lagacherie, P.; Coulouma, G. Regional Predictions of Eight Common Soil Properties and Their Spatial Structures from Hyperspectral Vis–NIR Data. Geoderma 2012, 189–190, 176–185.

79. Viscarra Rossel, R.A.; Webster, R. Predicting soil properties from the Australian soil visible–near infrared spectroscopic database. Eur. J. Soil Sci. 2012, 63, 848–860.

80. Vaudour, E.; Cerovic, Z.G.; Ebengo, D.M.; Latouche, G. Predicting Key Agronomic Soil Properties with UV-Vis Fluorescence Measurements Combined with Vis-NIR-SWIR Reflectance Spectroscopy: A Farm-Scale Study in a Mediterranean Viticultural Agroecosystem. Sensors 2018, 18, 1157.

81. Gholizadeh, A.; Saberioon, M.; Viscarra Rossel, R.A.; Boruvka, L.; Klement, A. Spectroscopic Measurements and Imaging of Soil Colour for Field Scale Estimation of Soil Organic Carbon. Geoderma 2020, 357, 113972.

82. Gomez, C.; Chevallier, T.; Moulin, P.; Bouferra, I.; Hmaidi, K.; Arrouays, D.; Jolivet, C.; Barthès, B.G. Prediction of Soil Organic and Inorganic Carbon Concentrations in Tunisian Samples by Mid-Infrared Reflectance Spectroscopy Using a French National Library. Geoderma 2020, 375, 114469.

83. Cremers, D.A.; Ebinger, M.H.; Breshears, D.D.; Unkefer, P.J.; Kammerdiener, S.A.; Ferris, M.J.; Catlett, K.M.; Brown, J.R. Measuring Total Soil Carbon with Laser-Induced Breakdown

Spectroscopy (LIBS). J. Environ. Qual. 2001, 30, 2202–2206.

84. Cécillon, L.; Baudin, F.; Chenu, C.; Houot, S.; Jolivet, R.; Kätterer, T.; Lutfalla, S.; Macdonald, A.; van Oort, F.; Plante, A.F.; et al. A Model Based on Rock-Eval Thermal Analysis to Quantify the Size of the Centennially Persistent Organic Carbon Pool in Temperate Soils. Biogeosciences 2018, 15, 2835–2849.